

# Conditions for practicing compressive Fresnel holography

Yair Rivenson<sup>1,\*</sup> and Adrian Stern<sup>2</sup>

<sup>1</sup>Department of Electrical and Computer Engineering, Ben-Gurion University of the Negev, P.O. Box 653, Beer-Sheva 84105, Israel

<sup>2</sup>Department of Electro-Optics Engineering, Ben-Gurion University of the Negev, P.O. Box 653, Beer-Sheva 84105, Israel

\*Corresponding author: rivenson@ee.bgu.ac.il

Received May 23, 2011; revised July 24, 2011; accepted August 3, 2011;  
posted August 4, 2011 (Doc. ID 148073); published August 23, 2011

Recent works have applied diffraction-based wave propagation for compressive imaging applications. In this Letter, we derive the theoretical bounds on the performance of compressive imaging systems based on Fresnel wave propagation, and we show that it is related to the imaging sensor's physical attributes, illumination wavelength, and working distance. © 2011 Optical Society of America

OCIS codes: 090.1995, 070.0070, 100.3190, 110.1758.

Recent works [1–7] have applied compressive sensing (CS) [8,9] operators based on free-space wave propagation and sparsity promoting image reconstruction from a hologram [10,11]. Using wave propagation as a sensing operator is appealing because it is closely related to the Fourier transform, which is often used as a sensing operator in CS [8]. In this Letter, we study the performance and limitations of CS systems based on wave propagation described by the Fresnel transform. The results are applicable for any type of holography, regardless of the recording setup.

For simplicity, let us consider 1D free-space propagation in the Fresnel approximation, which relates the complex values of a propagating wave measured in a plane perpendicular to the direction of propagation and separated by a distance  $z$  [12]:

$$\begin{aligned} u(\xi) &= u_{in} * \exp\left\{\frac{j\pi}{\lambda z} x^2\right\} \\ &= \exp\left\{\frac{j\pi}{\lambda z} \xi^2\right\} \int u_{in}(x) \exp\left\{\frac{j\pi}{\lambda z} x^2\right\} \exp\left\{\frac{-j2\pi}{\lambda z} \xi x\right\} dx, \end{aligned} \quad (1)$$

where  $u_{in}(x)$  is the input object,  $u(\xi)$  is the propagated field,  $\lambda$  is the wavelength, and  $z$  is the propagation distance of the light wave. The relation between the Fresnel transform and the Fourier transform is evident in Eq. (1). It is also clear that this relation depends on the distance  $z$ , suggesting that the applicability of the Fresnel transform as a sensing operator should also depend on  $z$ .

For the sake of clarity, let us give a brief review of CS. We assume that an image,  $\mathbf{u}$ , is composed of  $n$  pixels, but only  $s \ll n$  coefficients are meaningful under some arbitrary sparsifying operator,  $\Psi$ , such as a wavelet transform. We measure the signal using a sensing operator  $\Phi$  (the Fresnel transform in our case). This process is usually written in vector-matrix form:  $\mathbf{u}_{out} = \Phi \mathbf{u}$ , where  $\mathbf{u}_{out}$  has only  $m < n$  measurements, hence making the signal reconstruction an ill-posed problem. CS theory asserts that the signal can be accurately reconstructed when taking  $m$  uniformly at random selected measurements, obeying [9]

$$m \geq C\mu s \log n, \quad (2)$$

where  $\mu$ , which is referred to as the coherence parameter, measures the dissimilarity between the sensing operator,  $\Phi$ , and the sparsifying basis  $\Psi$ , and  $C$  is a positive numerical constant, which depends on the desired reconstruction accuracy [9]. The coherence parameter gets values of  $1 \leq \mu \leq n$ . Under the conditions of Eq. (2), an almost perfect signal reconstruction is guaranteed by performing an  $\ell_1$ -norm minimization procedure [8,9]. From Eq. (2) we notice that the smaller  $\mu$  is, the fewer samples are needed in order to reconstruct the underlying sparse image. The coherence parameter can also be interpreted as the amount of the spreading of the sparse input signal in the measurement domain, i.e., it is desired that each acquired sample will contain as much information as possible on the sensed (sparse) signal [9].

At large propagation distances, the Fresnel transform [Eq. (1)] can be approximated by a Fourier sensing operator (Fraunhofer approximation), which holds the lowest coherence possible;  $\mu = 1$  [9]. On the other hand, for  $z \rightarrow 0$ , the Fresnel transform behaves as an identity sensing operator, which gets the value of  $\mu = n$ .

Because CS practically uses a digital signal reconstruction procedure, from here on we refer to the numerical application of the Fresnel transform. The numerical Fresnel transform is one of the cornerstones of contemporary digital holography applications [13]. Traditionally, the numerical implementation of the Fresnel transform is divided into far-field (direct) and near-field (spectrum propagation) approximations [13,14]. These methods have very different numerical implementations, but each one of them is well suited for its own approximation regime.

In order to formulate the numerical evaluation of the Fresnel transform, we define  $\Delta x_0$  as the object resolution element size,  $\Delta x_z$  as the output field's pixel size, and  $n$  as the number of object and CCD pixels. For the numerical far-field regime, the Fresnel transform is evaluated by [13,14]

$$u(r\Delta x_z) = \exp\left\{j\pi \frac{r^2 \Delta x_z^2}{\lambda z}\right\} \mathbf{F} \left[ u(q\Delta x_0) \exp\left\{j\pi \frac{q^2 \Delta x_0^2}{\lambda z}\right\} \right], \quad (3)$$

where  $\mathbf{F}$  is the fast Fourier transform operator. When applying Eq. (3), we note that the relation between the input and output pixel sizes should be  $\Delta x_z = \lambda z / (n \Delta x_0)$ . Equation (3) is valid as an evaluation of the Fresnel transform for the working distance obeying [14,15]

$$z \geq z_0 = n \Delta x_0^2 / \lambda. \quad (4)$$

In order to comply with standard CS formulations, we shall rewrite Eq. (4) in a vector-matrix form:

$$\mathbf{u}_z = \mathbf{Q}_{\Delta x_z, z} \mathbf{F} \mathbf{Q}_{\Delta x_0, z} \mathbf{u} = \Phi^{FF} \mathbf{u}, \quad (5)$$

where  $\mathbf{Q}_{\Delta x_z, z}$  is a diagonal matrix such that the  $l$ th element on the diagonal is given by  $\exp\{j\pi l^2 \Delta x^2 / (\lambda z)\}$ . The matrix  $\Phi^{FF}$  stands for the far-field discrete sensing matrix. In the numerical far-field regime, the coherence parameter is actually equal to that of the Fourier transform, i.e.,  $\mu = 1$ . One of the ways to demonstrate this stems from considering the fact that  $\Phi^{FF}$  is actually an orthogonal transform. For randomly subsampling an orthogonal transform, the coherence parameter is given by the squared modulo of the largest entry of the sensing matrix [9], which can be easily calculated to show that  $\mu = n \max_{ij} |\Phi^{FF}|^2$ . An alternative argument, using the restricted isometry property, can be found in [16]. This result asserts that in the far-field regime, the distance *has no effect* on the sparse signal reconstruction guaranties, *and it behaves exactly as compressive Fourier sensing*. Consequently, from Eq. (2), the number of compressive samples, which are required to reconstruct the signal,  $m$ , is given by

$$m \geq Cs \log n. \quad (6)$$

Let us now examine the numerical near-field regime, i.e.,  $z < z_0$  [Eq. (4)]. In this case, the assumption is that the diffraction size does not change significantly, and we use the spectrum propagation method, also known as the convolution approach. In this case, the Fresnel transform is usually evaluated by

$$u_z(r \Delta x_z) = \mathbf{F}^{-1} \exp\left\{-j\pi \frac{\lambda z}{n^2 \Delta x_0^2} m^2\right\} \mathbf{F}\{u(l \Delta x_0)\}, \quad (7)$$

where  $\Delta x_z = \Delta x_0$ . As is done in the far-field regime, we shall rewrite Eq. (7) as a vector-matrix product, which is given by

$$\mathbf{u}_z = \mathbf{F}^{-1} \tilde{\mathbf{Q}}_{\Delta x_0, z} \mathbf{F} \mathbf{u} = \Phi^{NF} \mathbf{u}, \quad (8)$$

where  $\tilde{\mathbf{Q}}_{\Delta x_0, z}$  is a diagonal matrix with the  $l$ th element on the diagonal given by  $\exp\{-j\pi \lambda z l^2 / (n \Delta x_0)^2\}$ . The matrix  $\Phi^{NF}$  stands for the Fresnel near-field sensing matrix. A discrete convolution formulation of CS operators has been used before in several works [17,18], but these works considered the diagonal matrix as representing random phases, which is not so in our case. In a recent paper [9], the coherence parameter has been generalized for any type of convolution, not just random. In order to evaluate the coherence parameter of the convolution operator, [9] requires that the elements across the diagonal

of  $\tilde{\mathbf{Q}}_{\Delta x_0, z}$  will have the same magnitude. This of course holds true because  $|\exp\{-j\pi \lambda z l^2 / (n \Delta x_0)^2\}| = 1$  for every  $l$ . Then, [9] asserts that for a sensing matrix of the form

$$\Phi^{NF} = \begin{bmatrix} \phi(1) & \phi(n) & \dots & \phi(2) \\ \phi(2) & \phi(1) & \dots & \\ \vdots & \vdots & \ddots & \vdots \\ \phi(n) & \dots & \phi(2) & \phi(1) \end{bmatrix}, \quad (9)$$

the coherence parameter  $\mu = n \max_{ij} |\Phi^{NF}|^2 = n \max_r |\phi(r)|^2$ , because each column is a just a circularly shifted version of  $\phi(r)$ . We note that in our case,  $\phi(r)$  is actually the discrete Fresnel propagation point spread function (PSF). This means that in order to evaluate the coherence parameter, we need only to consider the maximum absolute value of the PSF (column), which is derived by substituting  $u(l \Delta x_0) = \delta(l \Delta x_0)$  in Eq. (7). The solution can be found in [13], and it states that the absolute value of the PSF,  $|\phi(r)|$ , slightly oscillates around the value of  $\Delta x_0 / (\lambda z)^{0.5}$ , as shown in Fig. 1. Although, as can be seen from Fig. 1, this value is strictly not  $\max_r |\phi(r)|$ , it is approximately the mean value of the oscillations, which in fact, should give a better representation for the convergence guaranties [17]. Therefore, the coherence parameter for the 1D case is given by the following:

$$\mu_{1D} = n \max_r |\phi(r)|^2 \approx n \frac{\Delta x_0^2}{\lambda z}. \quad (10)$$

For the 2D case, it can be shown [19] that

$$\mu_{2D} = \mu_{1D}^2 \approx n^2 (\max_r |\phi(r)|^2)^2 \approx N \left(\frac{\Delta x_0^2}{\lambda z}\right)^2 = \frac{N_F^2}{N}, \quad (11)$$

where  $N_F$  is the Fresnel number of a square aperture area of size  $(n \Delta x_0)^2$  [12] and  $N = n \times n$  denotes the total number of the 2D object pixels. Therefore, from Eqs. (2) and (11) and the number of compressive measurements required to accurately reconstruct the signal is given by the following:

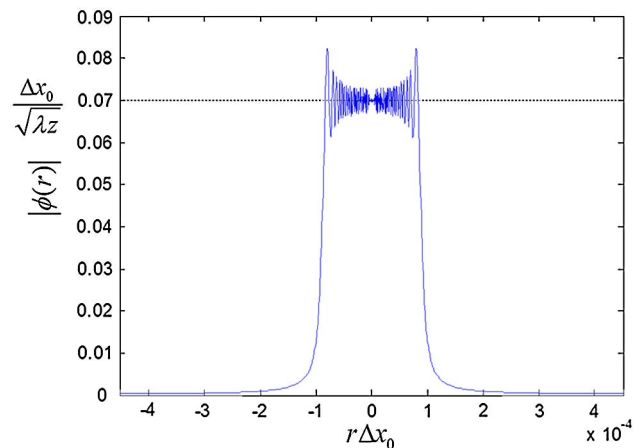


Fig. 1. (Color online) Numerical near-field evaluation of the Fresnel 1D PSF.

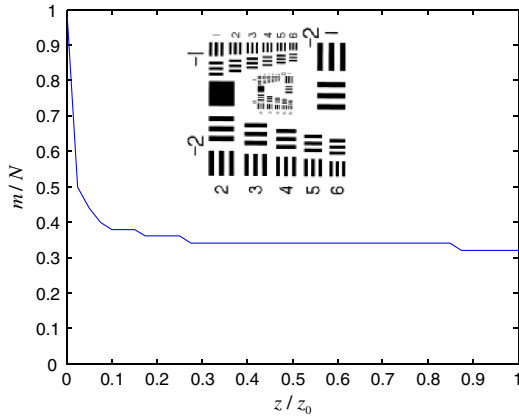


Fig. 2. (Color online) Simulation results showing the compressive sampling ratio required for reconstruction of the resolution target (inset) as a function of the working distance.

$$m \geq CN_F^2 \frac{s}{N} \log N = CN_F^2 \rho_s \log N, \quad (12)$$

where  $\rho_s = s/N$  is the density of the sparse image coefficients. Equation (12) works well with our physical intuition: the further we get from the object, the smaller the Fresnel number gets and the signal becomes more spread. From a CS perspective, each measurement contains more information about the object and the necessary number of compressive measurements required to accurately reconstruct the image decreases.

In the limit between the near- and far-field numerical evaluation regimes, i.e.,  $z = z_0$ , we obtain from Eqs. (4) and (11):

$$\mu_{2D}(z_0) = N \left( \frac{\Delta x_0^2}{\lambda z_0} \right)^2 = N \cdot \left( \frac{\Delta x_0^2}{\lambda(n\Delta x_0^2/\lambda)} \right)^2 = 1, \quad (13)$$

which is actually the lower bound for the coherence parameter and also its value for the numerical far-field approximation. We therefore obtain a continuous behavior of the coherence parameter for the entire span of the Fresnel approximation.

In order to demonstrate the results, we have performed a numerical experiment considering phase-shifting holography with the following parameters: pixel size of  $\Delta x_0 = 5 \mu\text{m}$  with 50% fill-factor,  $\lambda = 632.8 \text{ nm}$  and a  $1024 \times 1024$  pixel array, which dictates [Eq. (4)] the near-field evaluation to be valid for approximately  $z < 4 \text{ cm}$ . The object used is an intensity USAF 1951 resolution target (Fig. 2), which has the sparsity level of  $\rho_s = s/N \approx 0.08$  under the Haar wavelet transform. Noise was added such that the SNR level of the measured hologram was 25 dB. We have randomly chosen Fresnel samples for different  $z/z_0$  values and performed simulation to find the minimal number of compressive samples,  $m$ , required to obtain reconstruction with PSNR greater than 32 dB, which produced a satisfactory visual result. The reconstruction was carried out using the two-step iterative shrinkage/thresholding solver [20]. The results shown in Fig. 2 demonstrate that the CS ratio  $m/N$

decreases monotonically with the working distance till approaching asymptotically its minimal value in the far-field numerical regime ( $z \rightarrow z_0$ ). This was also demonstrated empirically in our previous work [21].

In conclusion, we have derived theoretical bounds for compressive Fresnel holography. We distinguished between the near- and far-field numerical approximations, which yield different behavior. The near-field numerical approximation regime dictates dependency between the minimal number of required compressive samples and the Fresnel number of the field's recording device, whereas for the numerical far-field evaluation, the CS ratio,  $m/N$ , is constant for every working distance and equals to that of the Fourier-based CS.

This research was partially supported by the Israel Science Foundation (ISF) under grant 1039/09 and Israel's Ministry of Science.

## References

1. D. J. Brady, K. Choi, D. L. Marks, R. Horisaki, and S. Lim, *Opt. Express* **17**, 13040 (2009).
2. M. M. Marim, M. Atlan, E. Angelini, and J.-C. Olivo-Marin, *Opt. Lett.* **35**, 871 (2010).
3. C. F. Cull, D. A. Wikner, J. N. Mait, M. Mattheiss, and D. J. Brady, *Appl. Opt.* **49**, E67 (2010).
4. Y. Rivenson, A. Stern, and B. Javidi, *J. Disp. Technol.* **6**, 506 (2010).
5. A. F. Coskun, I. Sencan, T.-W. Su, and A. Ozcan, *Opt. Express* **18**, 10510 (2010).
6. Y. Rivenson, A. Stern, and J. Rosen, *Opt. Express* **19**, 6109 (2011).
7. J. Hahn, S. Lim, K. Choi, R. Horisaki, and D. J. Brady, *Opt. Express* **19**, 7289 (2011).
8. E. Candes and M. Wakin, *IEEE Signal Process. Mag.* **25** (2), 21 (2008).
9. E. J. Candès and Y. Plan, "A probabilistic and RIPless theory of compressed sensing," *IEEE Trans. Inf. Theory* (to be published).
10. S. Soththivirat and J. A. Fessler, *J. Opt. Soc. Am. A* **21**, 737 (2004).
11. L. Denis, D. Lorenz, E. Thiébaud, C. Fournier, and D. Trede, *Opt. Lett.* **34**, 3475 (2009).
12. J. W. Goodman, *Introduction to Fourier Optics* (McGraw-Hill, 1996).
13. T. Kreis, *Handbook of Holographic Interferometry*, 1st ed. (Wiley-VCH, 2004).
14. D. Mas, J. Garcia, C. Ferreira, L. M. Bernardo, and F. Marinho, *Opt. Commun.* **164**, 233 (1999).
15. A. Stern and B. Javidi, *Opt. Eng.* **43**, 239 (2004).
16. D. L. Marks, J. Hahn, R. Horisaki, and D. J. Brady, in *IEEE International Conference on Computational Photography (ICCP) 2010* (IEEE, 2010), pp. 1–8.
17. J. Romberg, *SIAM J. Imaging Sci.* **2**, 1098 (2009).
18. Y. Rivenson, A. Stern, and B. Javidi, *Opt. Express* **18**, 15094 (2010).
19. Y. Rivenson and A. Stern, *IEEE Signal Process. Lett.* **16**, 449 (2009).
20. J. M. Bioucas-Dias and M. A. T. Figueiredo, *IEEE Trans. Image Process.* **16**, 2992 (2007).
21. Y. Rivenson and A. Stern, in *Computational Optical Sensing and Imaging*, OSA Technical Digest (CD) (Optical Society of America, 2011), paper CWB6.